Measurement of diffuse gamma ray at galactic plane by LHAASO-km2a

2021-08-24

张瑞[1]、赵世平[1 3]、张毅[1 2]、袁强[1] 、黄晓渊[1]

1.中科院紫金山天文台

2.中科院高能物理研究所

3.山东大学

OUTLINE

1. INTRO: Diffuse Gamma-ray Emission (DGE)

2. INTRO: LHAASO-KM2A Observation

3. Experimental data Selection

4. Diffuse emission analysis

1.INTRO: Diffuse Gamma-ray Emission (DGE)

Gamma-ray Sky Map

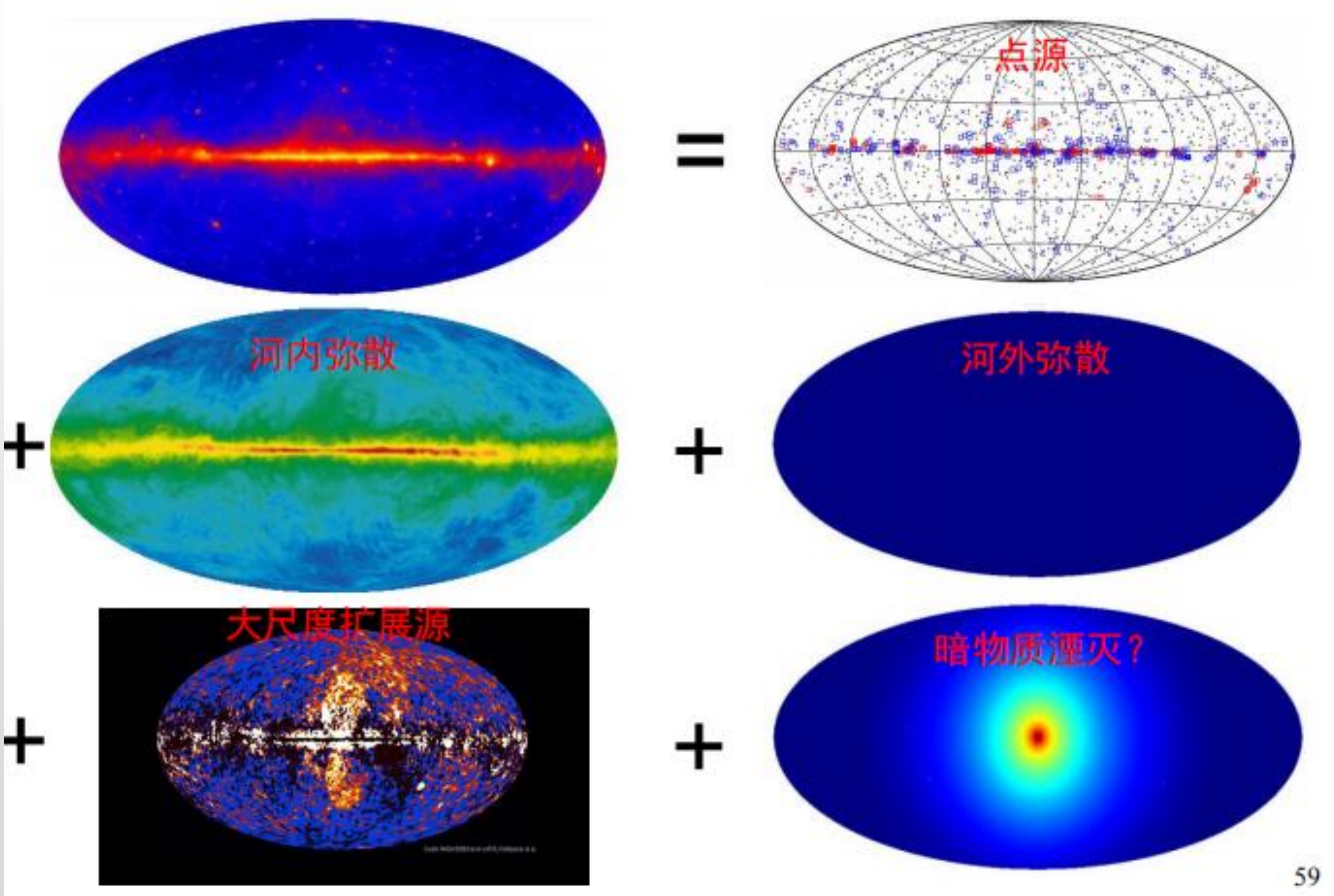

Sources of DGE from the Galactic plane

$$p, \alpha + ISM \rightarrow \pi^0 \rightarrow 2\gamma$$

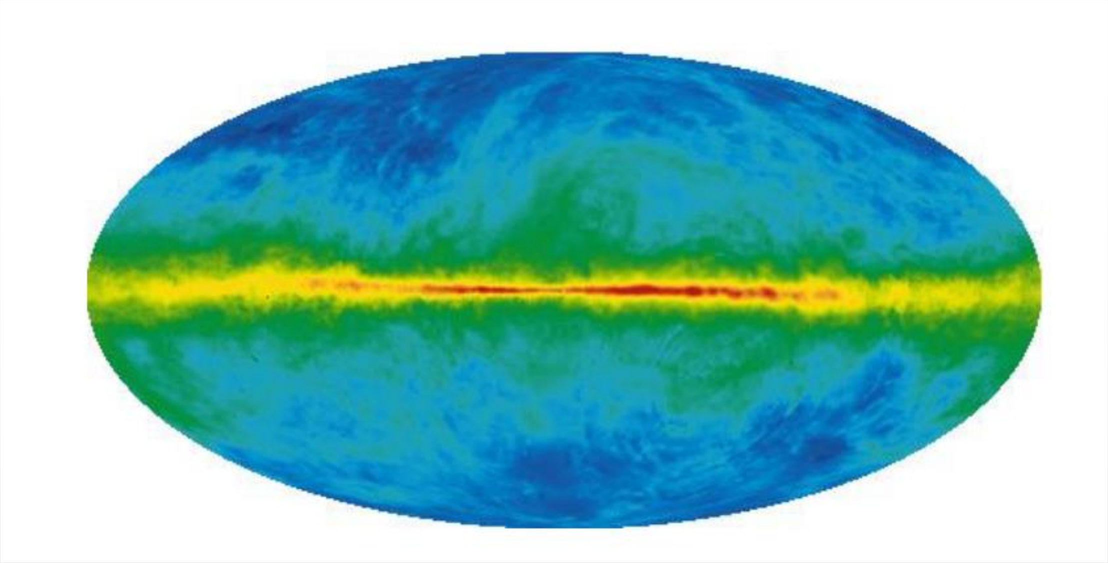

$$e + ISM \rightarrow \gamma$$ bremsstrahlung

$$e + ISRF \rightarrow \gamma$$ Inverse Compton scattering

- To study the propagation mechanism of cosmic rays;
- To study the material composition of Galactic plane;
- To search for dark matter annihilation signals;
- ...

Satellite Observation of DGE

- SAS-2 and COS B： first time
- COMPTEL and EGRET： **“GeV excess”**
- Fermi-LAT： high resolution

Fermi LAT Measurements of the Diffuse Gamma-Ray Emission at Intermediate Galactic Latitudes

Troy A. Porter* for the *Fermi* LAT Collaboration

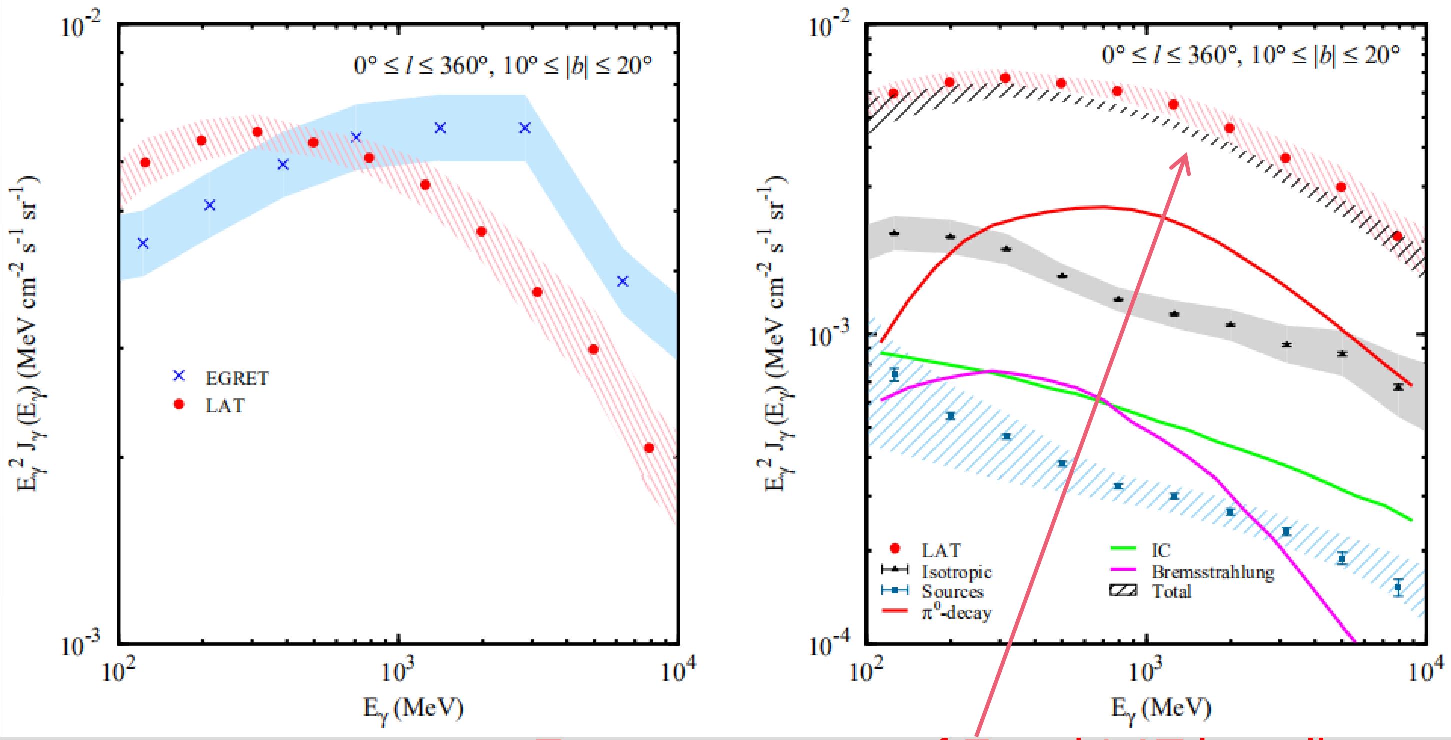

To explain "GeV excess":

- Harder cosmic ray injection spectrum;
- Contributions of unobserved point sources such as SNR;
- Scenes outside the Standard Model: dark matter particles annihilation;

Energy spectrum of Fermi-LAT is well reproduced by the DGE model

1.INTRO: Diffuse Gamma-ray Emission (DGE)

Ground Observation of DGE

Imaging Atmospheric Cherenkov Telescopes:

- Whipple and HEGRA
- H.E.S.S.

Diffuse Gamma Rays from the Galactic Plane: Probing the "GeV Excess" and Identifying the "TeV Excess"

Tijana Prodanović, Brian D. Fields[1]

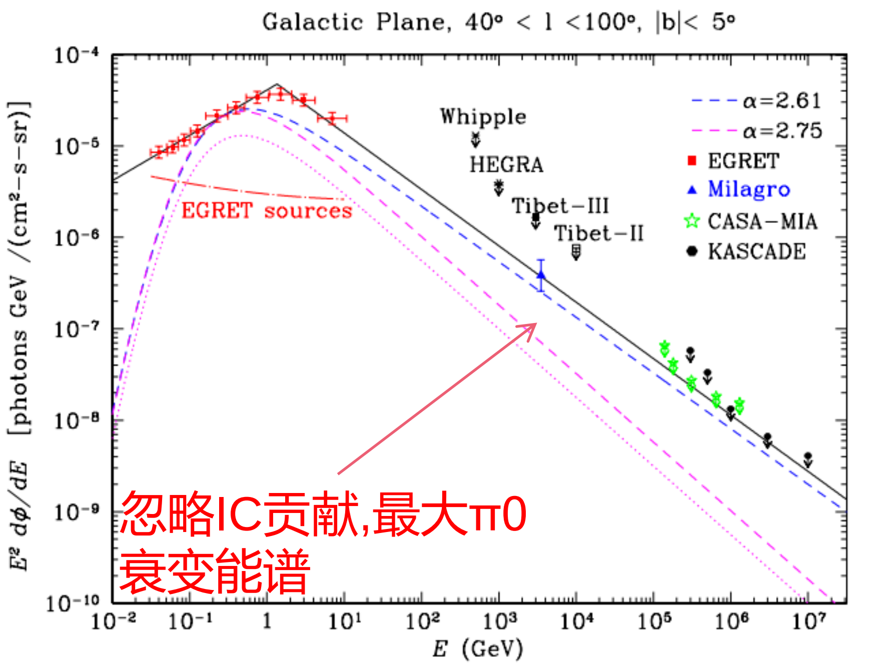

Air Shower Array:

- ASγ, KASCADE, CASA-MIA
- Milagro:**"TeV excess"**
- ARGO-YBJ
- ICECUBE
- LHAASO-KM2A

HEGRA(99% C.L., 38° < l < 43°, |b| < 2°);
Whipple (99.9% C.L., 38.5° < l < 41.5°, |b| <2°) ;
Tibet ASγ (99%C.L., 20° < l < 55°, |b| < 2°);
CASA-MIA(90%C.L.,50° < l < 200°, |b| < 5°);
KASCADE(90%C.L.,0° < ra < 360°, 14°<dec < 84°);

Search for PeV Gamma-Ray Emission from the Southern Hemisphere with 5 Years of Data from the IceCube Observatory

M. G. Aartsen,[16] M. Ackermann,[54] J. Adams,[16] J. A. Aguilar,[12] M. Ahlers,[20] M. Ahrens,[46] C. Alispach,[26]

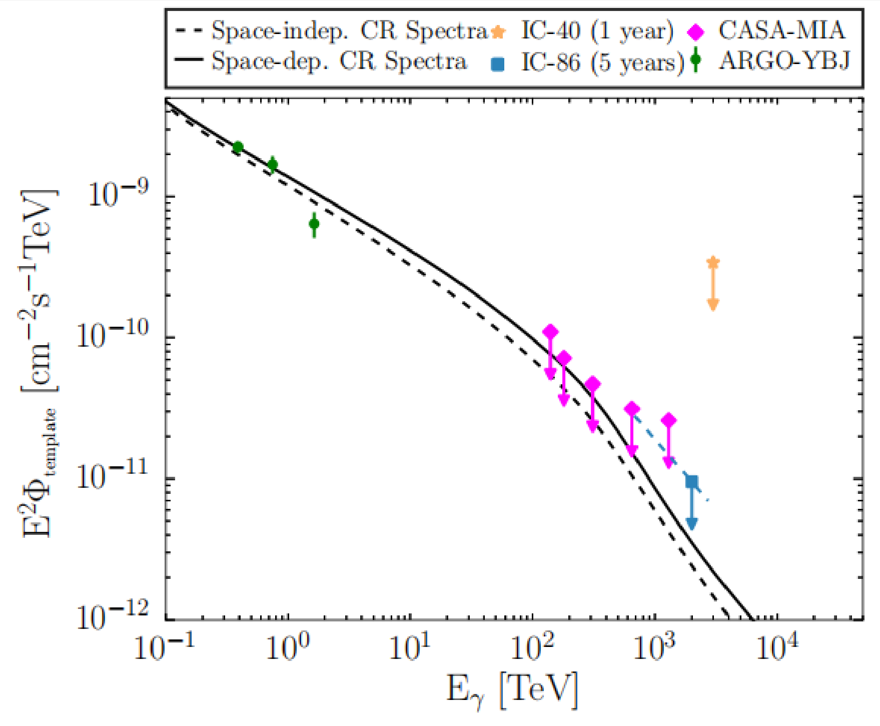

A Large area EAS array

covering 1.3 km^2

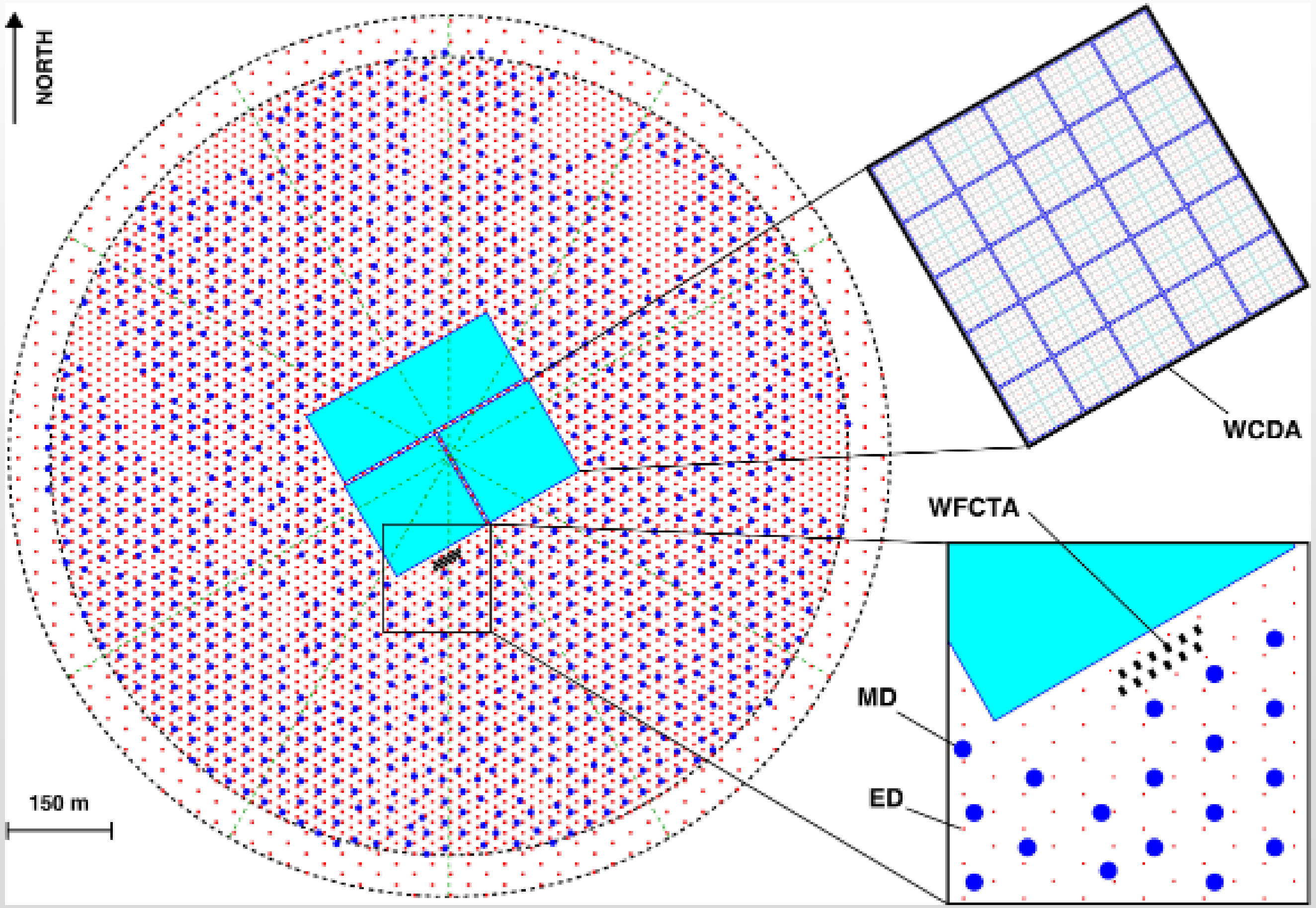

- **5195 EDs**
  - **1 m^2 each**
  - **15 m spacing**
- **1171 MDs**
  - **36 m^2 each**
  - **30 m spacing**
- **3120 WCDs**
  - **25 m^2 each**
- **18 WFCTs**

LHAASO:

- composition：KM2A、WCDA、WFCTA
- scientific targets： exploration of the origin of high-energy cosmic rays, scanning search for gamma sources, new physical phenomena, etc

-KM2A：

- Large field of view, High duty cycle
- Best range：>20TeV
- Search for new gamma sources
- Study on DGE

Gamma/Proton鉴别参数的确定(1)

$$R = log(\frac{N_\mu + 0.0001}{N_e}) \xrightarrow{\text{maximize}} Q = S/\sqrt{B}$$

logE:2.0-2.2

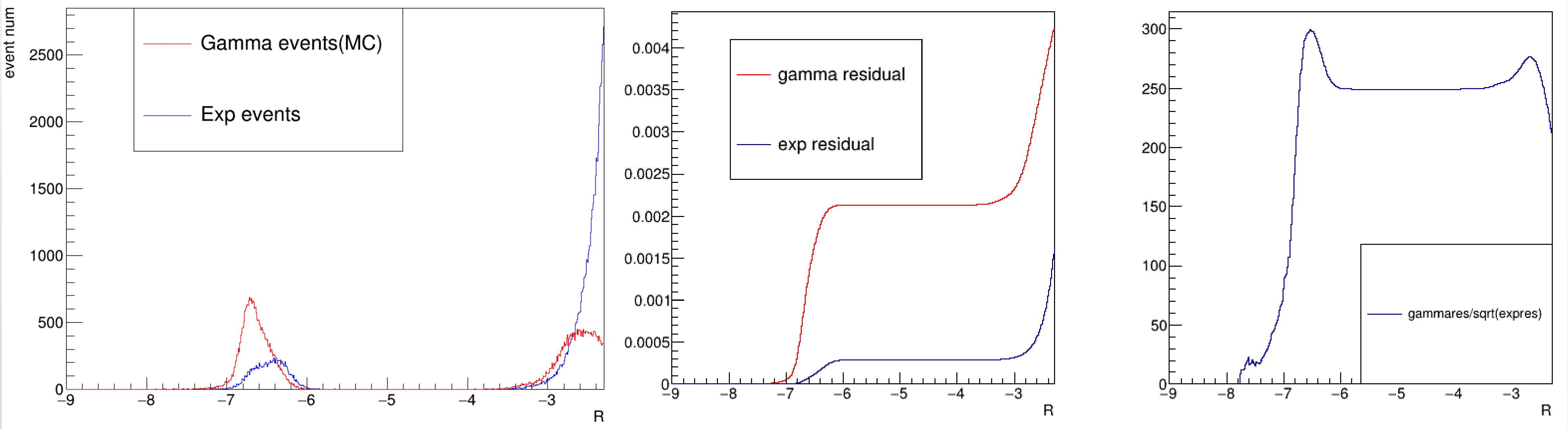

Gamma/Proton鉴别参数的确定(2)

$$R = log(\frac{N_\mu + 0.0001}{N_e})$$

$\log(E_{rec}/\mathrm{TeV})$	R for point-like source	R for DGE
1.0-1.2	-5.11	-5.00
1.2-1.4	-5.24	-3.20
1.4-1.6	-5.95	-5.96
1.6-1.8	-6.08	-6.17
1.8-2.0	-2.34	-2.50
2.0-2.2	-2.35	-2.69
2.2-2.4	-2.36	-2.79
2.4-2.6	-2.36	-2.74
2.6-2.8	-2.36	-2.75
2.8-3.0	-2.36	-2.79

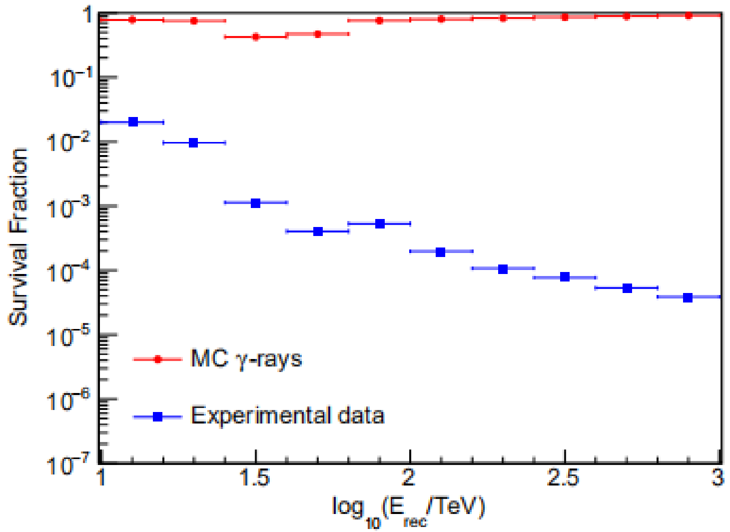

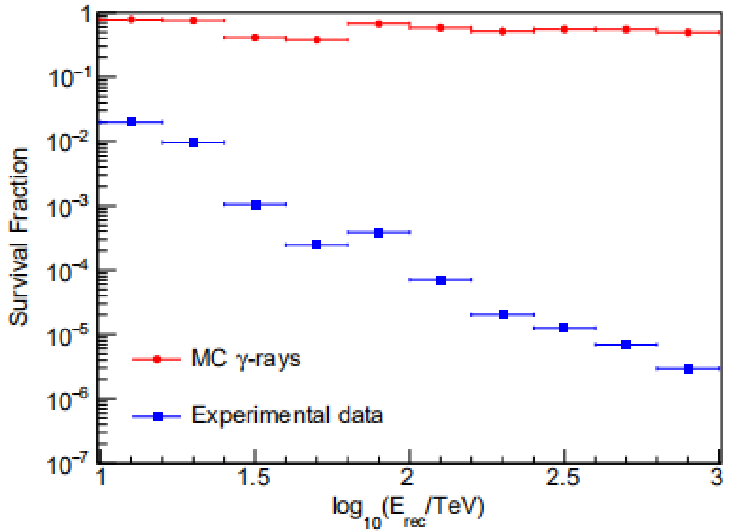

Gamma/Proton鉴别参数的确定(3)

Table 2: SED result of Crab at the rejection parameter R for DGE and for point-like source

Compare	Data time range	R	F20 $[TeV^{-1}\ cm^{-2}\ s^{-1}]$	γ
CPC crab	20191227-20200528	for point-like source	$1.13 \pm 0.05_{stat} \pm 0.08_{sys}$	$-3.09 \pm 0.06_{stat} \pm 0.02_{sys}$
This Work	20191227-20200528	for point-like source	1.12 ± 0.05	-3.10 ± 0.06
	20191227-20201130	for point-like source	1.06 ± 0.03	-3.14 ± 0.04
	20191227-20201130	for DGE	1.06 ± 0.03	-3.12 ± 0.04

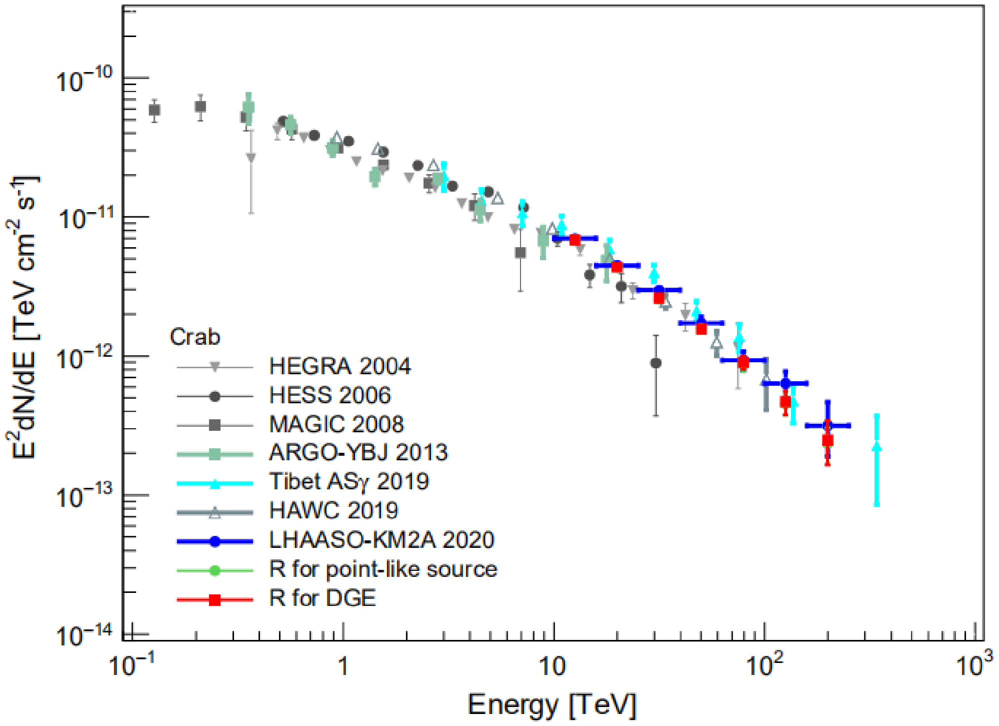

Background: Direct Integral method

- Efficiency of background change over time;
- "Mask" resolved sources and galactic plane;

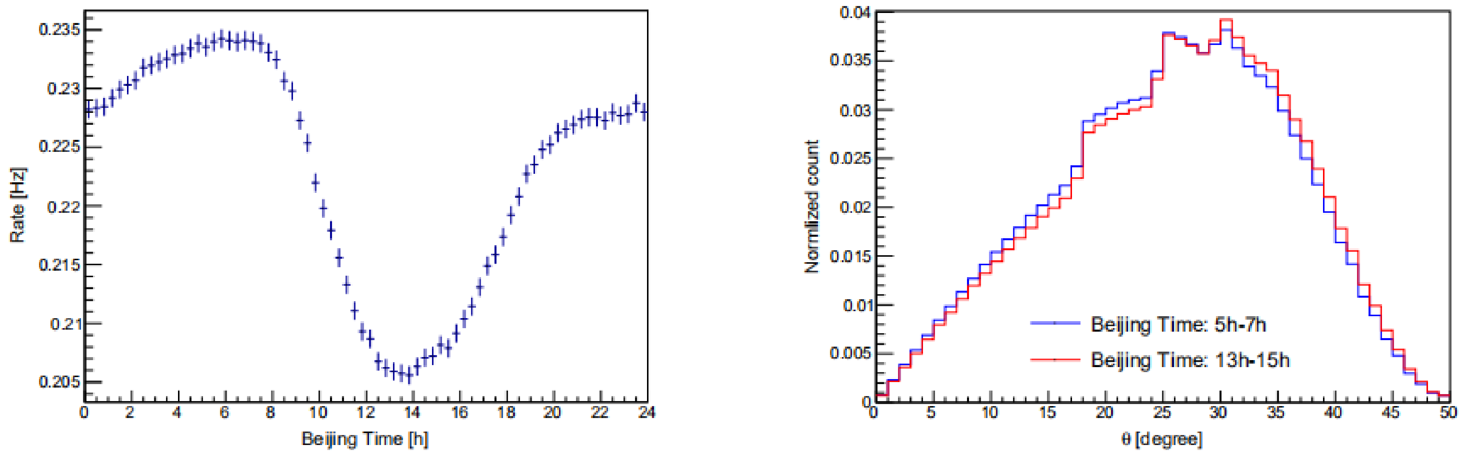

(a) (b)

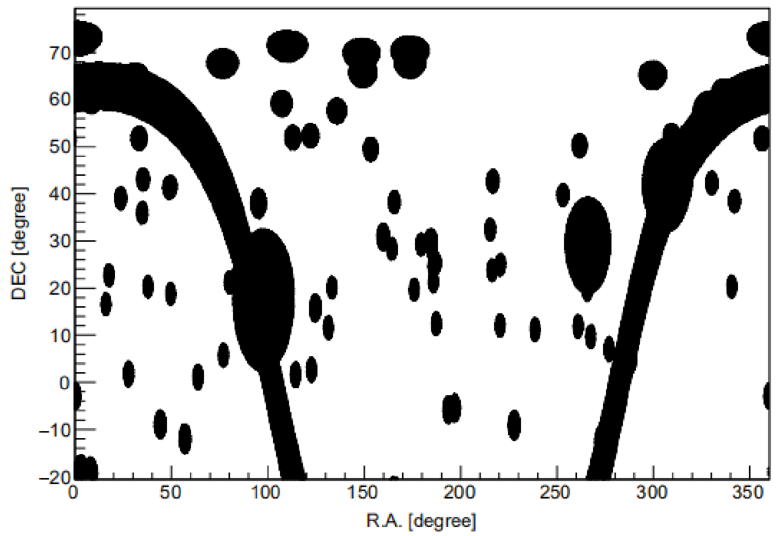

$$R_{mask} = NR \cdot \sqrt{psf^2 + ext^2}$$

$$R_{mask} = NR \cdot \sqrt{psf^2 + ext^2}$$

Subtraction of resolved sources(1)

MASK=A

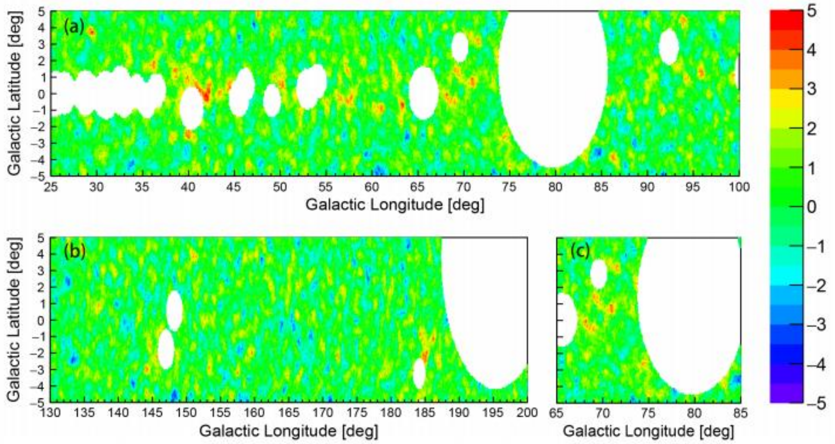

Fig. 13.— Model A: Sky Map with E_{rec} over 25TeV after mask as radius with Formula 2,where NR = 2. Model A assumes that the resolved sources signal is provided only by the sources in LHAASO catalogue. (a), (b) and (c) correspond to three study areas respectively.

MASK=B

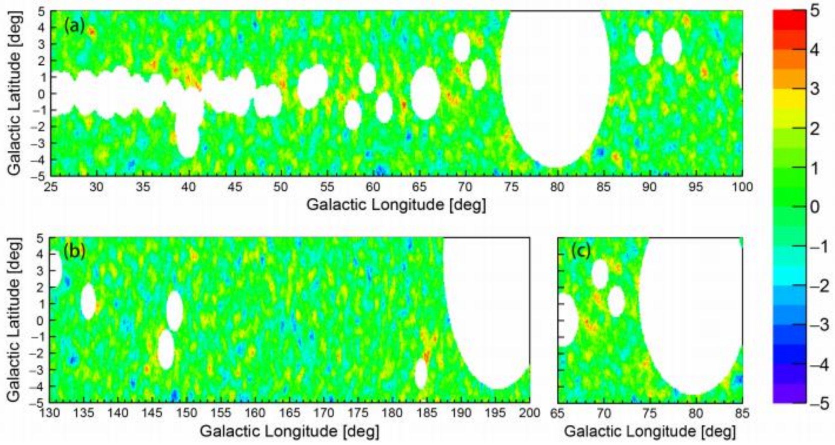

Fig. 14.— Model B: Sky Map with E_{rec} over 25TeV after mask as radius with Formula 2,where NR = 2. Model B assumes that the resolved sources signal is provided by the LHAASO cataloge sources plus TeVcat sources without LHAASO source counterpart. (a), (b) and (c) correspond to three study areas respectively.

Table 19: Preliminary LHAASO-KM2A source catalog at Galactic Plane above 25 TeV.

LHAASO Name	R.A. (deg)	Dec. (deg)	Sig.[a] (σ)	F^b_{20}	γ	Counterpart
Crab	83.63	22.02	38.2	10.6±0.3	-3.12 ± 0.04	Crab
J1839-057	279.86	-5.72	8.5	8.50 ± 0.99	-3.22 ± 0.13	HESS J1841-055
J1837-067	279.42	-6.74	5.7	8.05 ± 1.16	-3.45 ± 0.19	MAGIC J1835-069 MAGIC J1837-073 2HWC J1837-065 HESS J1837-069
J1843-036	280.93	-3.63	12.9	11.98 ± 0.90	-2.93 ± 0.08	HESS J1843-033 2HWC J1844-032 HESS J1844-030 HESS J1846-029
J1848-017	282.05	-1.73	5.6	7.12 ± 0.74	-3.31 ± 0.13	HESS J1848-018
J1848-000	282.20	-0.06	11.1	3.58 ± 0.69	-2.77 ± 0.19	IGR J18490-0000
J1851-000	282.98	-0.05	7.9	4.54 ± 0.72	-3.06 ± 0.15	IGR J18490-0000 HESS J1852-000
J1857+020	284.39	2.06	7.3	2.44 ± 0.43	-3.29 ± 0.19	HESS J1858+020
J1853+013	283.35	1.30	5.8	2.95 ± 0.52	-4.16 ± 0.27	2HWC J1852+013*
J1857+032	284.31	3.29	5.1	2.30 ± 0.36	-4.11 ± 0.26	MAGIC J1857.6+0297 HESS J1857+026 MAGIC J1857.2+0263
J1908+061	287.04	6.18	20.3	9.74 ± 0.53	-2.64 ± 0.06	MGRO J1908+06
J1915+110	288.92	11.04	5.7	2.32 ± 0.57	-2.68 ± 0.30	2HWC J1914+117* LHAASO-7[c]
J1914+120	288.52	12.01	5.2	0.96 ± 0.33	-2.68 ± 0.31	2HWC J1914+117*
J1923+141	290.78	14.17	5.1	1.25 ± 0.27	-3.27 ± 0.27	W 51
J1928+179	292.04	17.93	9.4	3.42 ± 0.37	-2.83 ± 0.11	2HWC J1928+177
J1928+190	292.13	19.05	8.8	1.71 ± 0.28	-2.91 ± 0.18	SNR G054.1+00.3
J1956+287	299.11	28.74	7.1	4.31 ± 0.39	-2.75 ± 0.09	2HWC J1953+294 2HWC J1955+285
J2019+367	304.87	36.78	28.6	9.75 ± 0.31	-2.93 ± 0.04	VER J2019+368 MGRO J2019+37
J2031+415	307.96	41.50	15.2	5.50 ± 0.31	-3.01 ± 0.07	MGRO J2031+41 PSR J2032+4127 TeV J2032+4130
J2108+519	317.25	51.98	8.9	1.65 ± 0.41	-2.67 ± 0.22	LHAASO J2108+519
J0341+529	55.39	52.94	6.2	1.99 ± 0.34	-2.87 ± 0.15	LHAASO-2[c]
J0357+539	59.49	53.99	4.8	2.17 ± 0.32	-3.63 ± 0.20	LHAASO-3[c]
J0542+236	85.71	23.69	5.5	0.89 ± 0.21	-3.26 ± 0.23	HAWC J0543+233
J1955+335	298.75	33.57	5.0	0.82 ± 0.19	-3.56 ± 0.29	LHAASO-13[c]
J2200+567	330.07	56.72	3.8	2.34 ±0.54	-3.07 ±0.20	LHAASO-11[c]

[a]Significance at the given source position after a top-hat smoothing.
[b]Flux at 20 TeV in unit of 10^{-15} TeV^{-1} cm^{-2} s^{-1}.
[c]LHAASO-num represents new sources discovered by LHAASO.

Subtraction of resolved sources(2)

$$R_{mask} = NR \cdot \sqrt{psf^2 + ext^2}$$

Table 3: Proportion (%) of residual signals of resolved sources to total signals

$\log(E_{rec}/\text{TeV})$	Inner Galaxy region		Outer Galaxy region		Cygnus region	
	Model A [a]	Model B [b]	Model A [a]	Model B [b]	Model A [a]	Model B [b]
1.0-1.2	6.79 ± 1.10	9.40 ± 1.90	3.96 ± 1.34	3.38 ± 2.58	2.59 ± 1.85	6.50 ± 3.11
1.2-1.4	6.25 ± 0.57	7.62 ± 0.81	0.99 ± 0.39	1.05 ± 0.84	4.10 ± 1.08	4.62 ± 0.84
1.4-1.6	3.32 ± 0.19	3.47 ± 0.11	0.49 ± 0.08	0.56 ± 0.04	3.62 ± 0.55	4.11 ± 0.17
1.6-1.8	2.44 ± 0.15	2.23 ± 0.06	0.56 ± 0.09	0.54 ± 0.07	2.69 ± 0.47	2.96 ± 0.08
1.8-2.0	2.52 ± 0.19	2.80 ± 0.09	0.33 ± 0.08	0.38 ± 0.05	4.19 ± 0.85	4.60 ± 0.19
>2.0	1.06 ± 0.10	0.81 ± 0.03	0.07 ± 0.03	0.03 ± 0.01	1.07 ± 0.50	0.65 ± 0.04

[a] Model A assumes that the resolved sources signal is provided only by the sources in LHAASO catalogue.

[b] Model B assumes that the resolved sources signal is provided by LHAASO catalogue sources plus TeVcat sources without LHAASO source counterpart.

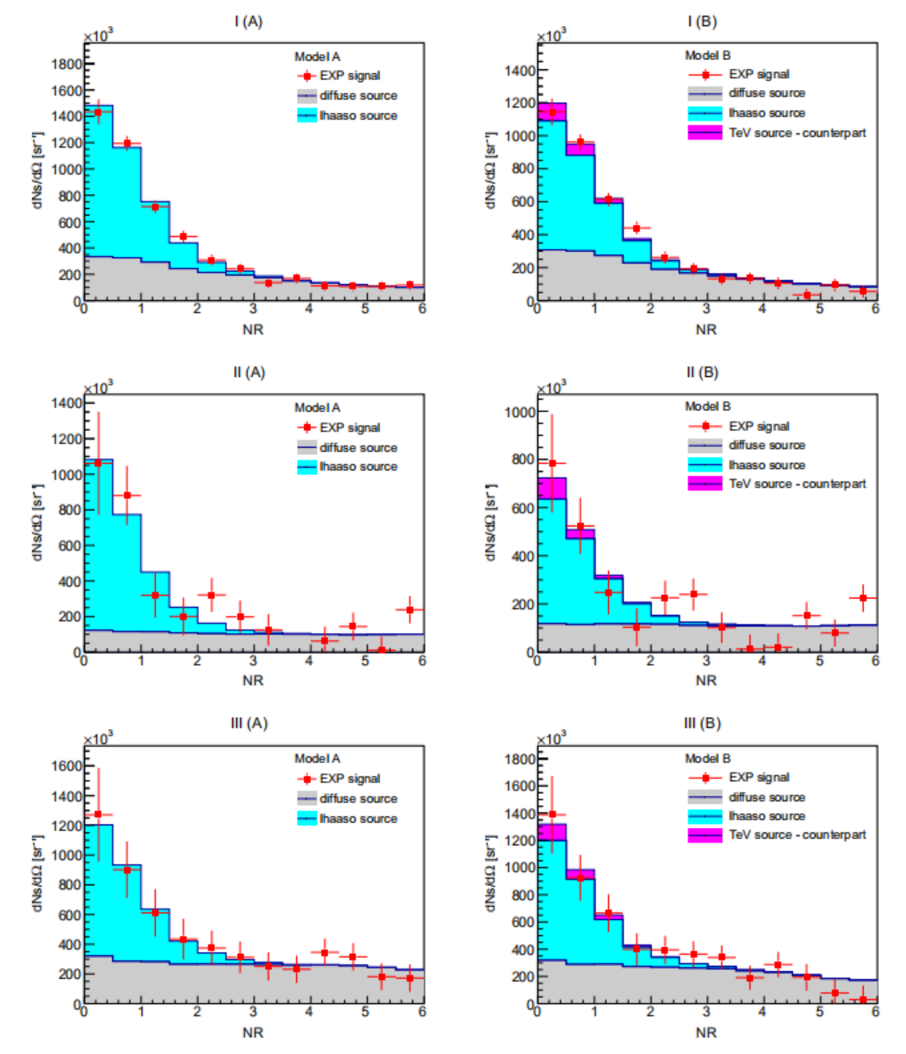

4. Diffuse emission analysis

$$\chi^2 = \sum_{i=1}^{n} \left(\frac{Ns_i - N_{MC_i}(\phi_0, \alpha)}{\sigma_{Ns_i}} \right)^2$$

Table 10: Fitting parameters of the LHAASO-KM2A DGE data.

	ϕ_0 (10^{-14} TeV^{-1} cm^{-2} s^{-1} sr^{-1})	α	Masking
Inner	1.71 ± 0.09	-3.00 ± 0.05	A
Outer	0.83 ± 0.10	-3.05 ± 0.15	A
Cygnus	2.00 ± 0.21	-3.17 ± 0.11	A
Inner	1.50 ± 0.10	-2.96 ± 0.06	B
Outer	0.82 ± 0.10	-3.07 ± 0.15	B
Cygnus	1.90 ± 0.40	-3.12 ± 0.12	B

MASK=A

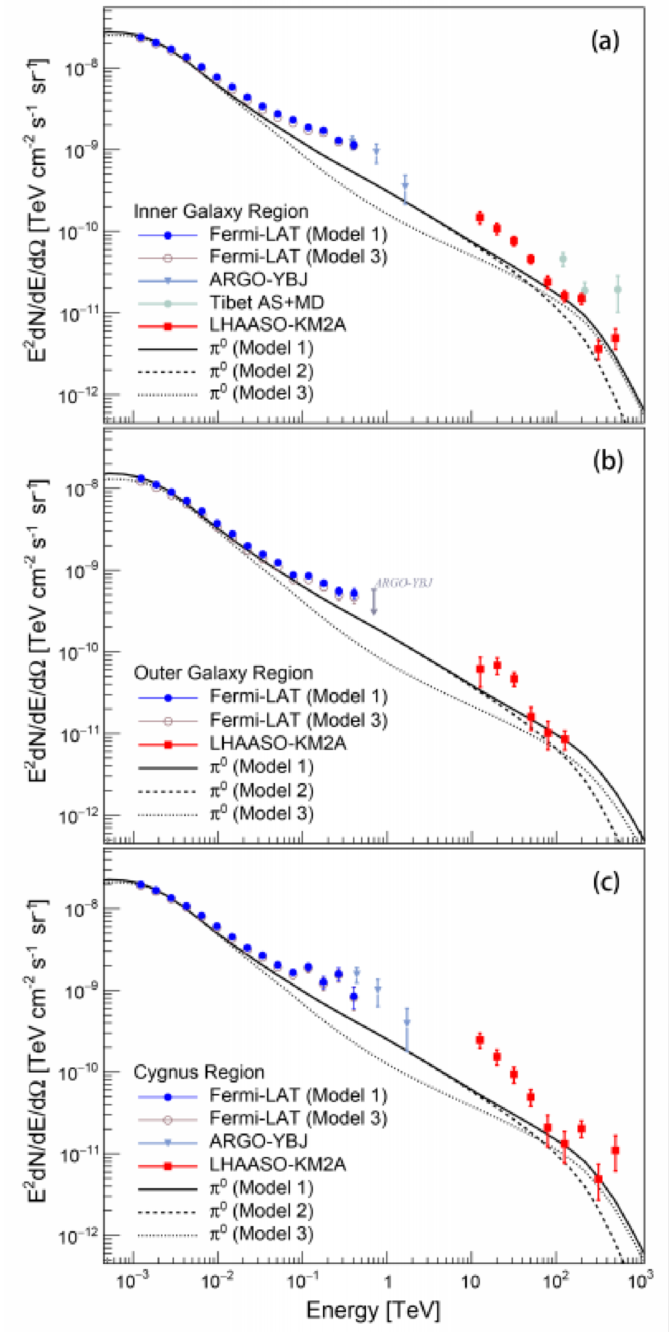

MASK=B

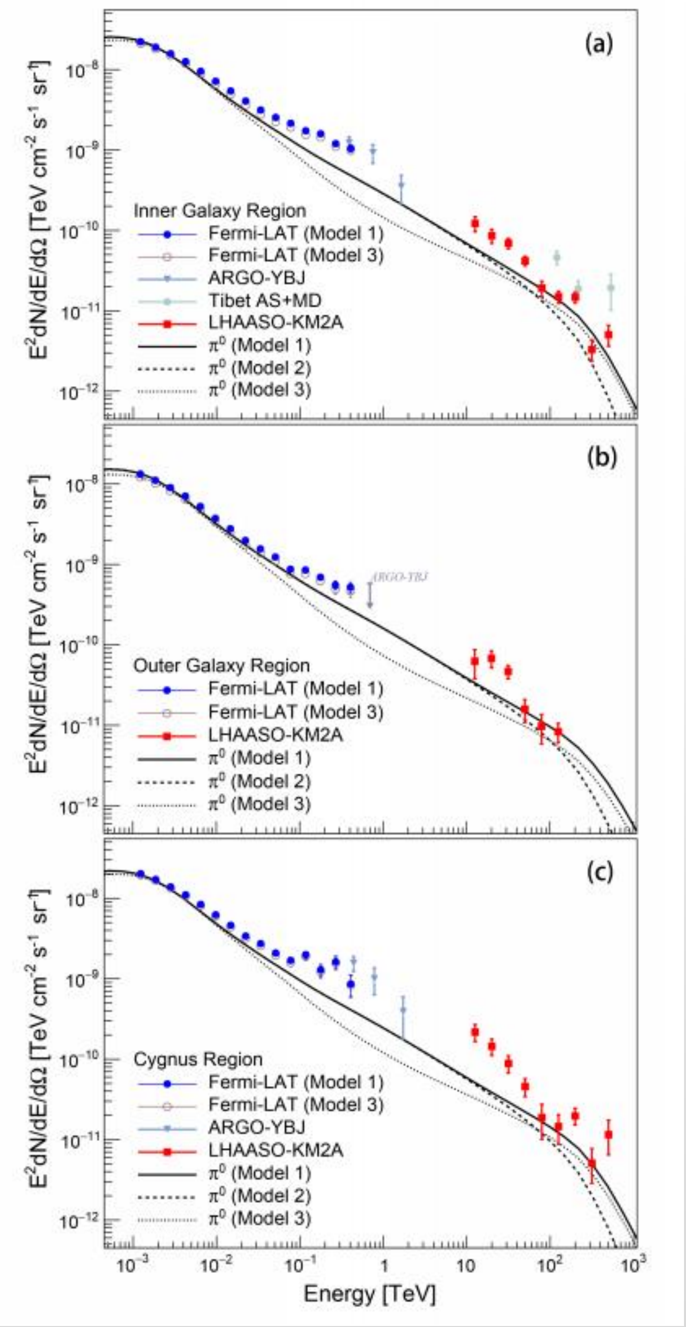

GL,GB distribution

MASK=A

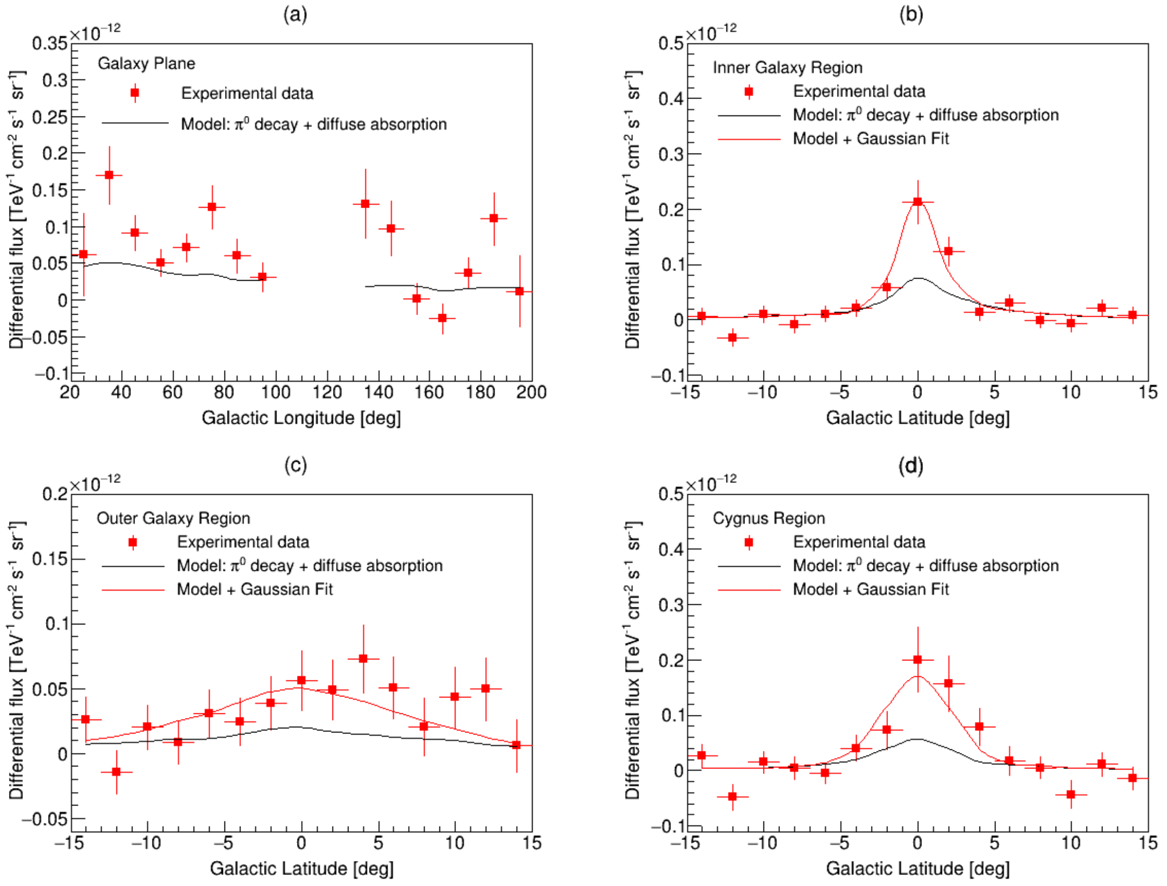

@31.6TeV

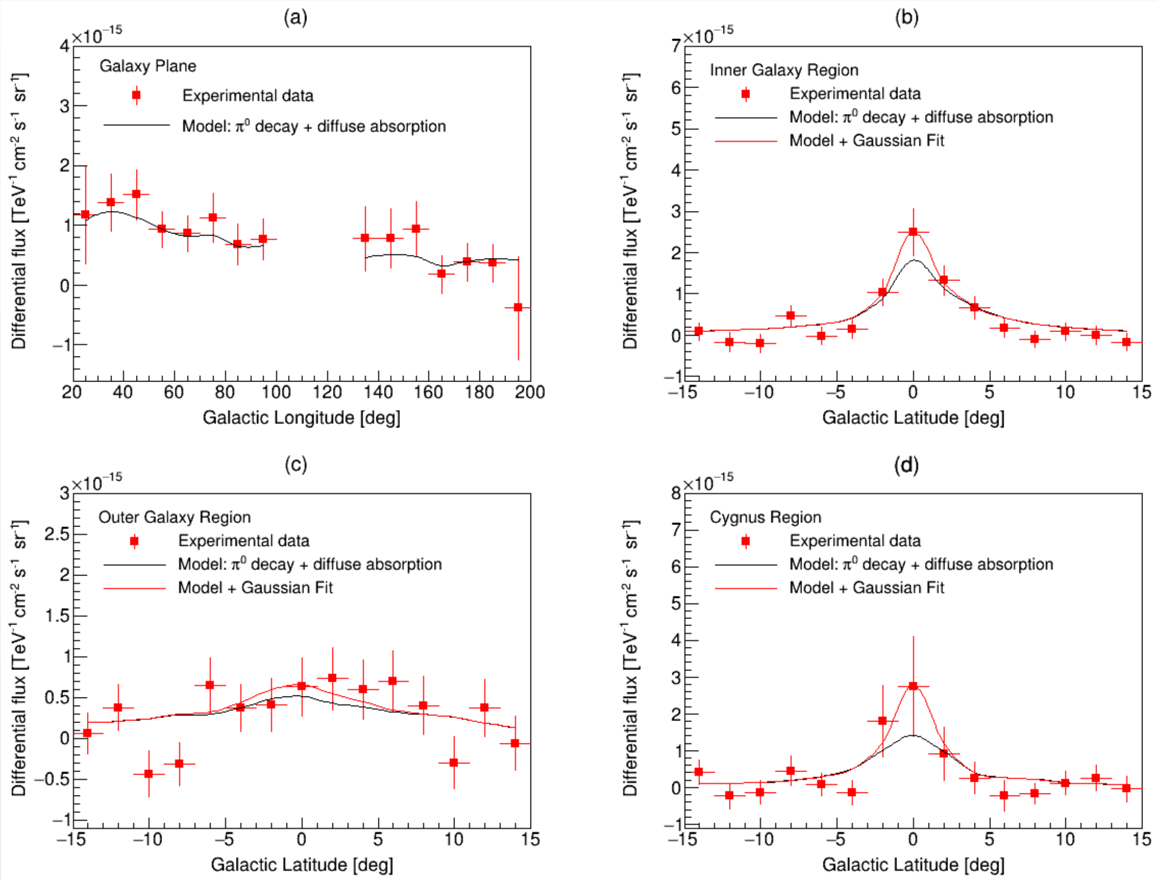

@126TeV

GL,GB distribution

MASK=B

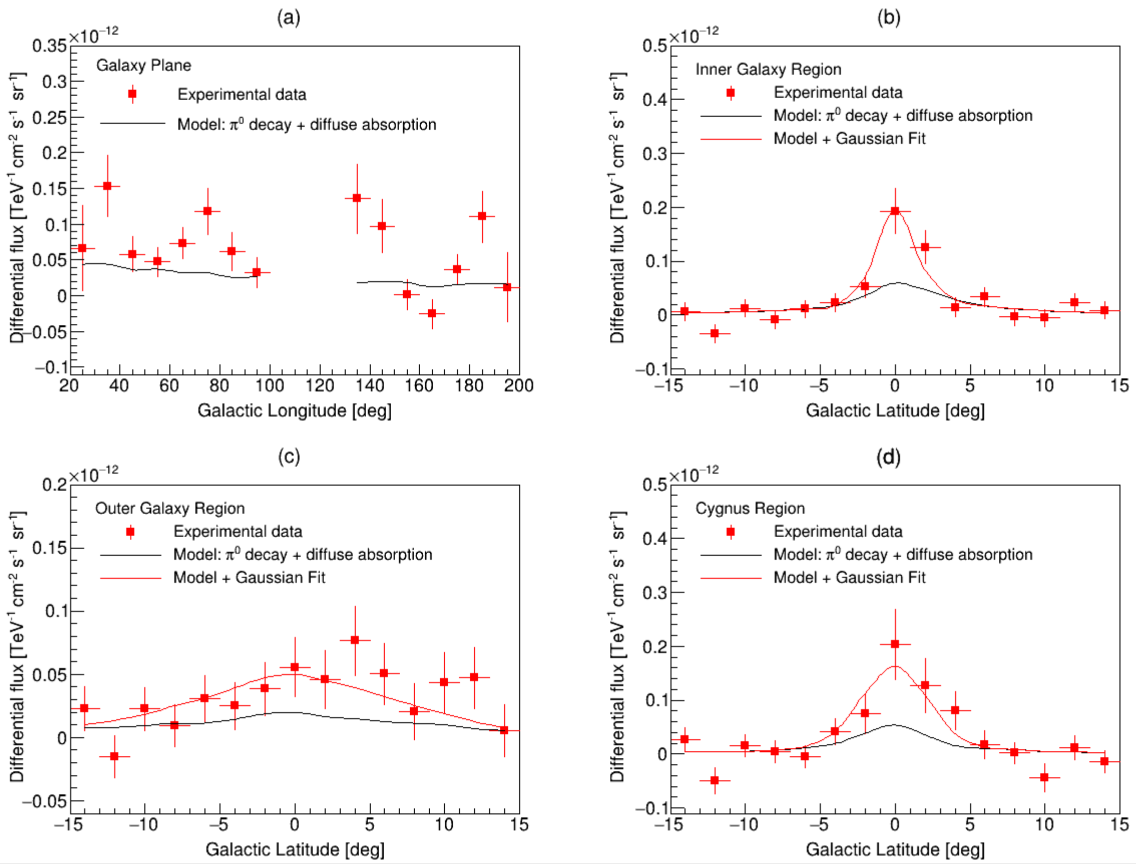

@31.6TeV

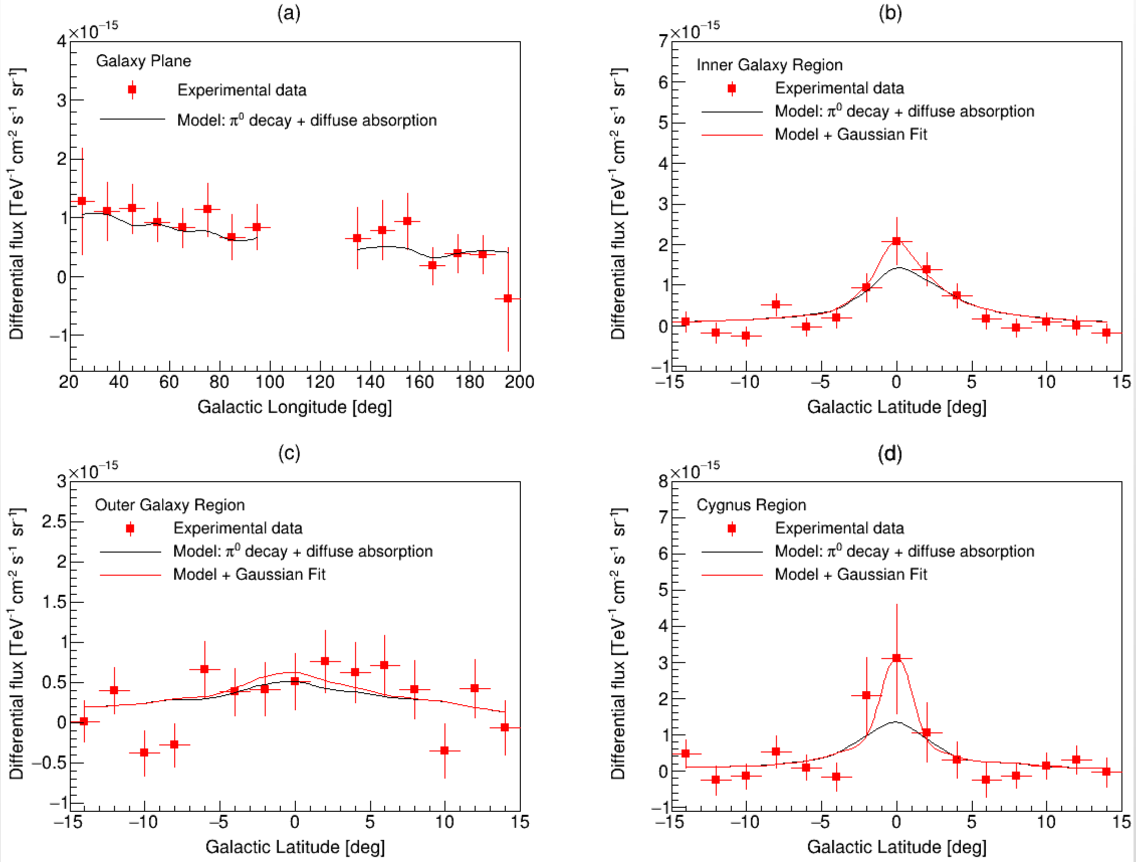

@126TeV

Check with ASγ

$$f(E) = (3.37 \pm 0.92) \times 10^{-14} \left(\frac{E}{50TeV}\right)^{-3.19 \pm 0.22}$$

- subtracting events within 0.5° from the known TeV sources.
- a new source LHAASO J2108+5157 with no TeV counterpart

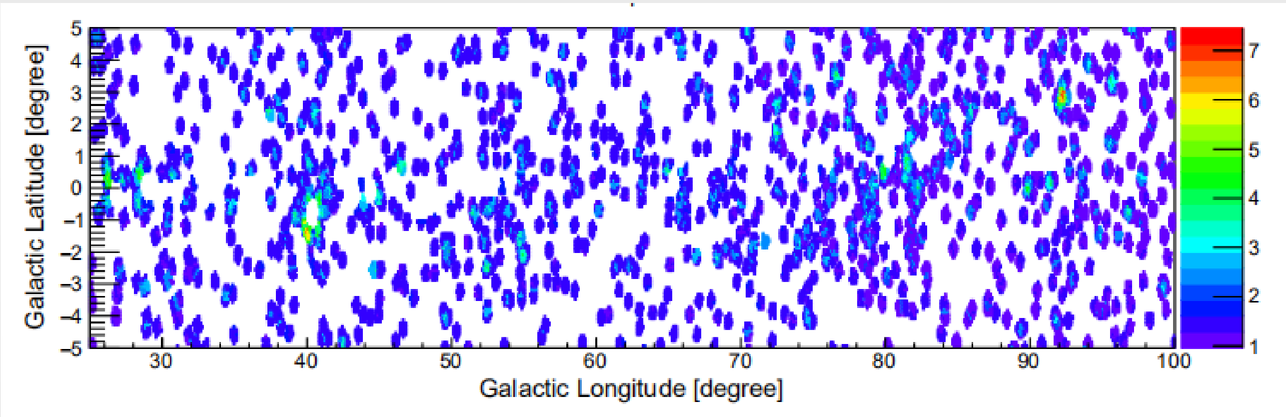

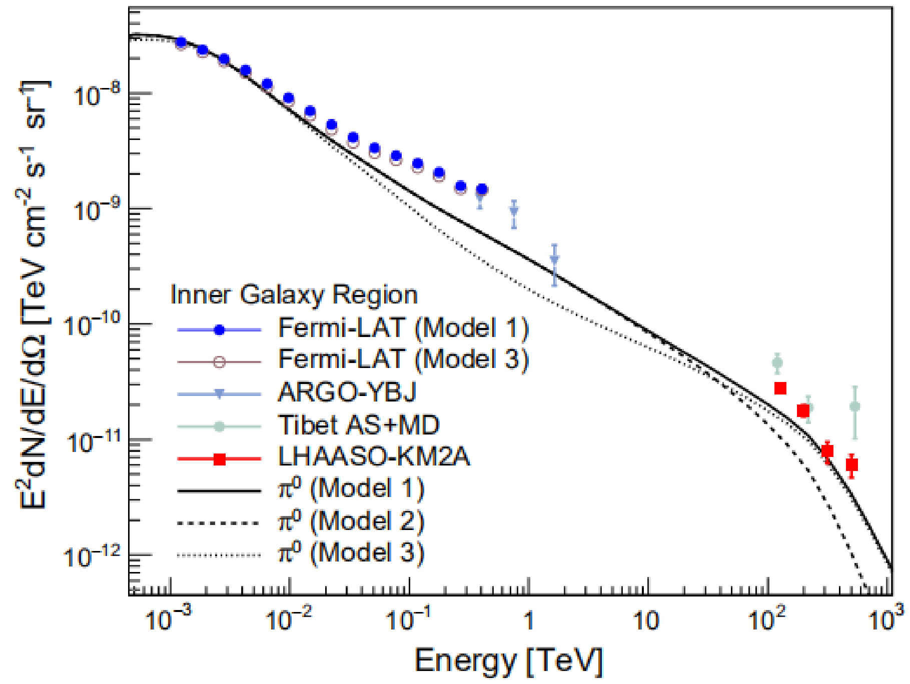

Systematic Uncertainties(1)

- layout;
- DI:Timerange? LST or MJD? Large Scale?
- atmospheric models

Table 12: systematic errors affecting the SED from detector layout

Mask model	Region	layout	F_{50} ($\mathrm{TeV^{-1}\ cm^{-2}\ s^{-1}\ sr^{-1}}$)	γ
A	I	layout1	$(1.71 \pm 0.09) \times 10^{-14}$	-3.00 ± 0.05
		layout2	$(1.71 \pm 0.09) \times 10^{-14}$	-3.01 ± 0.05
	II	layout1	$(8.27 \pm 1.00) \times 10^{-15}$	-3.05 ± 0.15
		layout2	$(8.25 \pm 1.00) \times 10^{-15}$	-3.07 ± 0.15
	III	layout1	$(2.00 \pm 0.21) \times 10^{-14}$	-3.17 ± 0.11
		layout2	$(1.97 \pm 0.20) \times 10^{-14}$	-3.19 ± 0.11
B	I	layout1	$(1.50 \pm 0.10) \times 10^{-14}$	-2.96 ± 0.06
		layout2	$(1.51 \pm 0.10) \times 10^{-14}$	-2.97 ± 0.06
	II	layout1	$(8.15 \pm 1.00) \times 10^{-15}$	-3.07 ± 0.15
		layout2	$(8.13 \pm 1.00) \times 10^{-15}$	-3.09 ± 0.15
	III	layout1	$(1.90 \pm 0.20) \times 10^{-14}$	-3.12 ± 0.12
		layout2	$(1.88 \pm 0.20) \times 10^{-14}$	-3.14 ± 0.11

Table 13: systematic errors affecting the SED from time range of efficiency reduction

Mask model	Region	Time range	F_{50} ($\mathrm{TeV^{-1}\ cm^{-2}\ s^{-1}\ sr^{-1}}$)	γ
A	I	10h	$(1.71 \pm 0.09) \times 10^{-14}$	-3.00 ± 0.05
		8h	$(1.74 \pm 0.09) \times 10^{-14}$	-2.99 ± 0.05
		6h	$(1.68 \pm 0.09) \times 10^{-14}$	-2.96 ± 0.05
		4h	$(1.66 \pm 0.09) \times 10^{-14}$	-2.93 ± 0.06
	II	10h	$(8.27 \pm 1.00) \times 10^{-15}$	-3.05 ± 0.15
		8h	$(7.92 \pm 1.00) \times 10^{-15}$	-3.06 ± 0.15
		6h	$(7.23 \pm 0.98) \times 10^{-15}$	-2.96 ± 0.17
		4h	$(7.24 \pm 0.98) \times 10^{-15}$	-2.96 ± 0.17
	III	10h	$(2.00 \pm 0.21) \times 10^{-14}$	-3.17 ± 0.11
		8h	$(2.00 \pm 0.21) \times 10^{-14}$	-3.17 ± 0.11
		6h	$(1.97 \pm 0.21) \times 10^{-14}$	-3.16 ± 0.12
		4h	$(2.00 \pm 0.20) \times 10^{-14}$	-3.14 ± 0.12
B	I	10h	$(1.50 \pm 0.10) \times 10^{-14}$	-2.96 ± 0.06
		8h	$(1.53 \pm 0.10) \times 10^{-14}$	-2.95 ± 0.06
		6h	$(1.47 \pm 0.10) \times 10^{-14}$	-2.92 ± 0.06
		4h	$(1.45 \pm 0.10) \times 10^{-14}$	-2.88 ± 0.06
	II	10h	$(8.15 \pm 1.00) \times 10^{-15}$	-3.07 ± 0.15
		8h	$(7.83 \pm 1.01) \times 10^{-15}$	-3.08 ± 0.15
		6h	$(7.14 \pm 0.98) \times 10^{-15}$	-2.99 ± 0.17
		4h	$(7.19 \pm 0.98) \times 10^{-15}$	-2.98 ± 0.17
	III	10h	$(1.90 \pm 0.20) \times 10^{-14}$	-3.12 ± 0.12
		8h	$(1.90 \pm 0.20) \times 10^{-14}$	-3.12 ± 0.12
		6h	$(1.87 \pm 0.20) \times 10^{-14}$	-3.10 ± 0.12
		4h	$(1.90 \pm 0.20) \times 10^{-14}$	-3.09 ± 0.12

Systematic Uncertainties(2)

- layout;
- DI:Timerange? LST or MJD? Large Scale?
- atmospheric models

Table 13: systematic errors affecting the SED from time scale

Mask model	Region	Time Scale	F_{50} (TeV^{-1} cm^{-2} s^{-1} sr^{-1})	γ
A	Inner	MJD	$(1.71 \pm 0.09) \times 10^{-14}$	-3.00 ± 0.05
		LST	$(1.71 \pm 0.09) \times 10^{-14}$	-3.03 ± 0.06
	Outer	MJD	$(8.27 \pm 1.00) \times 10^{-15}$	-3.05 ± 0.15
		LST	$(8.09 \pm 0.99) \times 10^{-15}$	-3.06 ± 0.14
	Outer	MJD	$(2.00 \pm 0.21) \times 10^{-14}$	-3.17 ± 0.11
		LST	$(1.96 \pm 0.20) \times 10^{-14}$	-3.17 ± 0.11
B	Inner	MJD	$(1.50 \pm 0.10) \times 10^{-14}$	-2.96 ± 0.06
		LST	$(1.51 \pm 0.10) \times 10^{-14}$	-2.98 ± 0.06
	Outer	MJD	$(8.15 \pm 1.00) \times 10^{-15}$	-3.07 ± 0.15
		LST	$(7.98 \pm 0.99) \times 10^{-15}$	-3.08 ± 0.14
	Cygnus	MJD	$(1.90 \pm 0.20) \times 10^{-14}$	-3.12 ± 0.12
		LST	$(1.86 \pm 0.20) \times 10^{-14}$	-3.10 ± 0.12

- atmospheric models(CPC Crab):

The influence on Flux is less than 7%;
and the influence on index is around 0.02;

Table 14: systematic errors affecting the SED from large-scale structure introduced by direct integration method

Mask model	Region	Large-scale Structure Correction	F_{50} (TeV^{-1} cm^{-2} s^{-1} sr^{-1})	γ
A	Inner	before	$(1.71 \pm 0.09) \times 10^{-14}$	-3.03 ± 0.06
		after	$(1.75 \pm 0.09) \times 10^{-14}$	-3.04 ± 0.05
	Outer	before	$(8.09 \pm 0.99) \times 10^{-15}$	-3.06 ± 0.14
		after	$(7.18 \pm 0.99) \times 10^{-15}$	-3.07 ± 0.15
	Cygnus	before	$(1.96 \pm 0.20) \times 10^{-14}$	-3.17 ± 0.11
		after	$(2.12 \pm 0.40) \times 10^{-14}$	-3.15 ± 0.20
B	Inner	before	$(1.51 \pm 0.10) \times 10^{-14}$	-2.98 ± 0.06
		after	$(1.55 \pm 0.10) \times 10^{-14}$	-3.00 ± 0.06
	Outer	before	$(7.98 \pm 0.99) \times 10^{-15}$	-3.08 ± 0.14
		after	$(7.10 \pm 0.99) \times 10^{-15}$	-3.09 ± 0.15
	Cygnus	before	$(1.86 \pm 0.20) \times 10^{-14}$	-3.10 ± 0.12
		after	$(1.97 \pm 0.40) \times 10^{-14}$	-3.14 ± 0.22

Table 15: Fitting parameters of the LHAASO-KM2A DGE data.

	ϕ_0 (10^{-14} TeV^{-1} cm^{-2} s^{-1} sr^{-1})	α	Masking
Inner	$1.71 \pm 0.09_{stat} \pm 0.13_{sys}$	$-3.00 \pm 0.05_{stat} \pm 0.06_{sys}$	A
Outer	$0.83 \pm 0.10_{stat} \pm 0.15_{sys}$	$-3.05 \pm 0.15_{stat} \pm 0.10_{sys}$	A
Cygnus	$2.00 \pm 0.21_{stat} \pm 0.22_{sys}$	$-3.17 \pm 0.11_{stat} \pm 0.04_{sys}$	A
Inner	$1.50 \pm 0.10_{stat} \pm 0.12_{sys}$	$-2.96 \pm 0.06_{stat} \pm 0.05_{sys}$	B
Outer	$0.82 \pm 0.10_{stat} \pm 0.15_{sys}$	$-3.07 \pm 0.15_{stat} \pm 0.09_{sys}$	B
Cygnus	$1.90 \pm 0.40_{stat} \pm 0.18_{sys}$	$-3.12 \pm 0.12_{stat} \pm 0.06_{sys}$	B

Systematic Uncertainties(3)

- Take mask type（A or B） into Systematic Uncertainties

Table 16: Fitting parameters of the LHAASO-KM2A DGE data.

	ϕ_0 (10^{-14} TeV^{-1} cm^{-2} s^{-1} sr^{-1})	α
Inner	$1.71 \pm 0.09_{stat} \pm 0.25_{sys}$	$-3.00 \pm 0.05_{stat} \pm 0.07_{sys}$
Outer	$0.83 \pm 0.10_{stat} \pm 0.15_{sys}$	$-3.05 \pm 0.15_{stat} \pm 0.10_{sys}$
Cygnus	$2.00 \pm 0.21_{stat} \pm 0.24_{sys}$	$-3.17 \pm 0.11_{stat} \pm 0.06_{sys}$